

Symmetry-aware Registration of Human Faces

Martin Prantl, Libor Váša and Ivana Kolingerová

NTIS - New Technologies for the Information Society, Faculty of Applied Sciences, University of West Bohemia,
Technická 8, Pilsen, Czech Republic

Keywords: Registration, Symmetry, Computer Graphics.

Abstract: Registration of 3D objects is a challenging task, especially in presence of symmetric parts. A registration algorithm based on feature vectors must be able to distinguish left and right parts. Symmetric geometry can be found in those two parts, however, most popular feature vectors produce equal numbers in this case, even though the geometry is in fact different. One field, where this problem arises, is the registration of partially overlapping parts of human faces or entire heads. The symmetric parts in this case are often eyes, ears, nostrils, mouth corners etc. Using symmetry-oblivious feature vectors makes it hard to distinguish left and right part of the face or head. This paper presents a feature vector modification based on a vector field flux and curvature. Results show that the modified feature vector can improve the subsequent registration process.

1 INTRODUCTION

Global registration of partially overlapping parts of the same model is a well-known problem in the field of computer graphics and geometry processing. An object is scanned from several viewpoints, which leads to several partially overlapping data sets. The goal is to find transformations that align these data sets and obtain a complete model. To register data sets, overlapping areas have to be found.

A commonly used approach consists of two main steps - first, a simplified description of local neighborhoods is created, and then it is used to find a transformation that aligns the parts. A simplified description is essential for the speed of algorithms. From the points of simplified description *feature vectors* (or descriptors) are created. They essentially hold condensed information about the neighborhood. For example, the vector can be created using information from local angles, curvatures, normal vectors, distances, colors etc.

In the second step, the created feature vectors are used to find similar parts, based on the difference of the corresponding feature vectors (euclidean distance or dot product of normalized feature vectors can be used for this purpose). Identified similar parts are then used to find a transformation that aligns them. The alignment is often not accurate, and may be further improved by a local registration algorithm, such as Iterative Closest Point (ICP).

The quality and success of the registration depends on the amount of details in the input data as well as on the amount of information included in the feature vector. The vectors should be *descriptive*, i.e. they should vary with varying local shape, they should be resilient to noise, and they should be *invariant* to translation and rotation. Scale invariance is usually not required, because the parts are mostly scanned at the same scale. The scale, translation and rotation invariance can be jointly achieved by enforcing isometry invariance. Such an approach, although commonly used, has a fundamental flaw: isometries include reflections, and reflections represent a *relevant change* of local shape, which should not be ignored. However, to the best of our knowledge, descriptors are not created to be symmetry aware. For example, ears of a human head are pair, symmetric organs. The results from existing state-of-the-art descriptors indicate that a local shape of a left ear is *identical* to the local shape of the right ear, since there exists an isometry that maps one to the other. The isometry, however, includes a reflection, and in fact left ear *cannot* be well aligned with the right one.

Scanning of human faces is quite common recently. An automated registration based on current state-of-the-art methods often fails to find the correct transformation for aligning the partial scans. In this article, we propose an algorithm that improves an existing feature vector by adding symmetry information. Although human faces are not fully symmetric, from

the registration point of view the symmetry plays an important role.

The proposed algorithm is based on the current state-of-the-art method Fast Global Registration (FGR) by Zhou et al. (Zhou et al., 2016). This approach uses the FPFH descriptor (Rusu et al., 2009). We have improved this feature vector by adding the symmetry information. The proposed feature vector modification can be used with other registration algorithms as well. Our proposed solution fits directly into other existing pipelines, since only the feature vector is changed and the rest of the registration process remains unaffected.

The rest of this paper is organized as follows: Section 2 covers current state-of-the-art methods in feature vectors for geometry registration. Section 3 explains the proposed solution. Section 4 presents the algorithm results. Section 5 concludes the paper.

2 RELATED WORK

There are many existing state-of-the-art algorithms for feature vector computation. A comprehensive comparison of feature vectors was recently done by Guo et al. in (Guo et al., 2016). Authors compare several properties of feature vectors and their goal is to determine which descriptor is suitable for which type of data. However, no symmetric data were included in the experiments.

The second part of the registration process is to find the transformation. Usually, the algorithms that propose a novelty in a feature vector construction also offer the description of the registration process based on the proposed feature vector. However, it is not necessary and a feature vector can be used with other registration algorithms as well.

Majority of methods use statistics based on normal vector or curvature. Other solutions can be based on Euclidean distances ((Maximo et al., 2011)), voxelization ((Knopp et al., 2010)), Fourier transform ((Foulds and Drevin, 2011)) etc.

Neural networks can also be used for registration purposes. One general approach was proposed by Liu et al. (Liu et al., 2006). Another solution for a large scene and small parts that are being registered inside the scene was presented by Elbaz et al. (Elbaz et al., 2017). A global disadvantage of neural network based solutions is the need for a training set that can be sometimes hard to obtain. Therefore, solutions based on feature vectors computed from the geometry are often preferred.

Solutions primarily based on normal vector statistics can be found in (Drost et al., 2010; Rusu et al.,

2009; Tombari et al., 2010) etc. Some of these algorithms are implemented in the PCL library. Their basic overview can be found in (Holz et al., 2015).

Tombari et al. (Tombari et al., 2010) extend a 2D image descriptor SIFT (Lowe, 2004) to 3D. The resulting descriptor is called SHOT. The algorithm uses normal vectors of points to construct a reference frame. Based on it, the neighborhood is divided into several 3D spherical volumes. Each volume has its own histogram created from angles between normals of points and the normal at the center point.

A descriptor based on the so-called *spin image* (Johnson and Hebert, 1999) creates the feature vector by projection of points from 3D to 2D. For each point, other points in the neighborhood of a given radius are projected to 2D. A scale invariant method, based on spin images, has been proposed by (Lin et al., 2017).

A frequently used descriptor is Fast Point Feature Histogram (FPFH). It was proposed by Rusu et al. (Rusu et al., 2009). The descriptor is based on the relationships between points in a neighborhood of a certain radius and the estimated surface normals. The points in the neighborhood are paired, and based on the changes in orientations of their local coordinate systems in each pair, a histogram is created and used as the descriptor of the neighborhood. The simplicity, low number of elements in the final feature vector and high performance make FPFH very often the first choice when selecting a descriptor.

Jiaqi et al. (Jiaqi et al., 2016) use not only normal vectors, but also the density of points in neighborhood and local depths. They create an overall histogram based on all of these properties. The histogram is used as a feature vector. Approaches based on surface curvature estimation can be used without the need of having normal vectors. Curvature can be computed by integral invariants (Pottmann et al., 2007) which is a solution based on a voxelization algorithm. A descriptor using this curvature calculation was presented by Gelfand et al. (Gelfand et al., 2005). The computed curvature, after normalization, is used to obtain descriptors on the model surface. Interesting parts of the models are found using a histogram of curvature. The most important parts of the model are the ones, where rare curvature values occur.

A solution based on a local voxelization has been presented by Knopp et al. (Knopp et al., 2010). Their solution is a 3D variant of 2D feature descriptor SURF (Bay et al., 2008). The geometry is voxelized using the intersection of mesh faces with the volume raster. A saliency measure is computed using a process similar to image convolution for each cell of the volume.

3 THE PROPOSED ALGORITHM

Solutions presented in section 3 yield the same feature vector for the symmetric, yet not identical parts of the same object, leading to an incorrect registration - see Figure 1c.

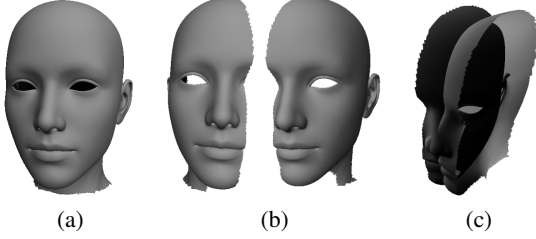


Figure 1: a) Original data of a human head; b) Left and right part of the human head; c) An incorrect registration of the two parts.

We propose two approaches to distinguishing left and right parts in models involving symmetries. The first approach is based on interaction of the local shape with a strongly orientation dependent vector field. The second approach is based on curvature estimation and a local coordinate system created in the directions of the normal vectors and the extremal curvatures. Both versions lead to a signed value that represents flux direction or signed volume. Based on the sign, we can distinguish symmetric geometry parts.

3.1 Vector Field

Our first approach is based on analyzing the local shape using a symmetry-aware vector field. Having a surface and a vector field that goes through it, we can calculate the flux. It describes the quantity which passes through a surface and based on the direction of the vector field and orientation of the surface, it has either positive or negative sign. We can utilize this knowledge to distinguish orientation of the local surface. Symmetric parts will have opposite signs and this can be used for the feature vector modification.

The initial derivation is based on a triangle mesh, however, this approach can be used for point clouds as well. First, we describe the solution based on a triangle mesh and later explain its modification for a point cloud.

3.1.1 Triangle Mesh

We want to calculate the feature vector at a vertex P (equipped with the normal vector n_p) of an input triangle mesh. We define a vector field as a vector function

$$v(X) = (P - X) \times n_p, \quad (1)$$

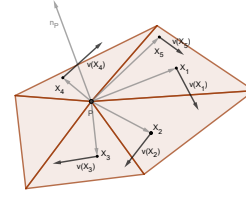


Figure 2: A local neighborhood with a few sample points X_i and vector field values at them.

The entire setup with a few points X_i can be seen in Figure 2.

Our goal is to integrate the dot product of this field with triangle normals over all neighboring triangles. For i -th triangle, we compute the following integral:

$$F_i = \int_{\Delta_i} v(X) \cdot n_i d\Delta_i, \quad (2)$$

where n_i is the normal of the i -th triangle. Finally, we sum these values over all triangles in a local neighborhood as

$$F_s = \sum_i F_i,$$

Points X in a triangle can be parameterized by scalars r and s as:

$$X = A_i + r(B_i - A_i) + s(C_i - A_i), \quad (3)$$

where A_i , B_i and C_i are vertices of the triangle that contains X , $r \in \mathbb{R}$ and $s \in \mathbb{R}$ are parameters fulfilling the conditions $r + s = 1$ and $r, s \geq 0$.

To calculate the integral (2), we have to change the bounds of the integral. From the integral over the area of triangle Δ_i , we get the integral based on the previously defined parametric function in Equation (3) with parameters r and s :

$$F_i = \int_{r=0}^1 \int_{s=0}^{1-r} v(A_i + r(B_i - A_i) + s(C_i - A_i)) \cdot n_i J_i ds dr, \quad (4)$$

where J_i is the Jacobian associated with the change of the integral bounds and it is equal to $J_i = \|(B_i - A_i) \times (C_i - A_i)\|$. The integral from Equation 4 can be rewritten using Equations 1 and 3 to:

$$F_i = J_i \int_{r=0}^1 \int_{s=0}^{1-r} (P \times n_p \cdot n_i - A_i \times n_p \cdot n_i - r(B_i - A_i) \times n_p \cdot n_i - s(C_i - A_i) \times n_p \cdot n_i) ds dr. \quad (5)$$

To simplify Equation 5, we use a substitution:

$$\begin{aligned} \alpha_i &= (P - A_i) \times n_p \cdot n_i, \\ \beta_i &= -(B_i - A_i) \times n_p \cdot n_i, \\ \gamma_i &= -(C_i - A_i) \times n_p \cdot n_i, \end{aligned} \quad (6)$$

which leads to

$$F_i = J_i \int_{r=0}^1 \int_{s=0}^{1-r} (\alpha_i + \beta_i r + \gamma_i s) ds dr \quad (7)$$

$$= \frac{1}{6} J_i (3\alpha_i + \beta_i + \gamma_i).$$

After the removal of substitution from Equation 6, we end up with a solution

$$F_i = \frac{1}{2} J_i (P - T_i) \times n_p \cdot n_i, \quad (8)$$

where T_i is a centroid of a triangle $A_i B_i C_i$, i.e. calculated as $T_i = \frac{1}{3}(A_i + B_i + C_i)$.

If we compute the triangle normal t_i as $(B_i - A_i) \times (C_i - A_i)$, then Equation 8 can be further simplified to

$$F_i = \frac{1}{2} (P - T_{A_i B_i C_i}) \times n_p \cdot [(B_i - A_i) \times (C_i - A_i)], \quad (9)$$

3.1.2 Point Cloud Modification

Application to point clouds without connectivity is possible if we interpret the data as a dual representation. We can think of the input points as centroids of virtual triangles, while the actual vertices are unknown. The idea is visualized in Figure 3: Figure 3a shows the standard way, where points P_i (blue color) of the cloud are taken as vertices of triangles and centroids (green color) are calculated from them, Figure 3b shows the dual interpretation, where the points P_i (blue color) are used as centroids directly.

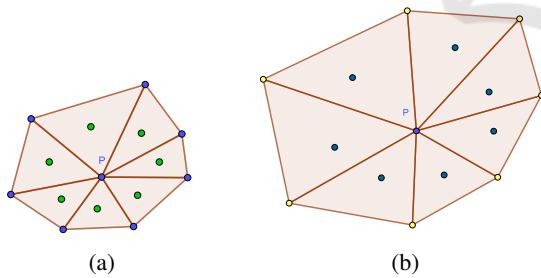


Figure 3: a) Point cloud P_i (blue points) as triangulation with green centroids of triangles; b) Points P_i of cloud (blue points) are used as centroids of “virtual” triangles. The yellow points are just for illustration of one possible “virtual” triangulation of the neighborhood.

For the point cloud modification, the overall triangulation is not required. We use only points P_i with their normal vectors that are used as normal vectors of the “virtual” triangles. The result can be improved if we have available non-normalized normal vectors that hold the information about the area of virtual triangle. This is similar to the Jacobian in the triangle

mesh solution. If unit-length normal vectors are used, the virtual triangles are considered to have equal area. Based on this, we can directly use the Equation 9 and get the final solution for a point cloud as:

$$F_i = \frac{1}{2} (P - P_i) \times n_p \cdot n_i.$$

The result is influenced by the size of the neighborhood that is obtained by a nearest-neighbor search within a threshold distance. A comparison of different neighborhood sizes is shown in Figure 4, which shows the point cloud modification. Near similar results were acquired using a triangle mesh, and therefore they are not included. It can be seen that with the increasing neighborhood size, the results become more stable. The sign of the obtained values does not unambiguously identify the right/left side, however, this is actually not our goal. More importantly, parts differing only by a symmetry have a different sign and can therefore be distinguished.

3.2 Curvature

The second proposed approach is based on curvature estimation. It can be used for a triangle mesh or a point cloud. There are many algorithms for a curvature estimation (for a recent survey, see (Váša et al., 2016)) and the selection of one depends on estimation circumstances, such as type of input data, quality of the input, required performance and others. Noise in input data can lead to problems with curvature. However, due to targeting on human faces, the input data can be partially smoothed out which limits the noise level. The smoothing process can remove wrinkles and other imperfections, but they are not important for the registration.

Given the points of an input point cloud, where we want to calculate a feature vector, for every point P (equipped with the normal vector n) we find its neighborhood. The size of the neighborhood can be selected. We have used the same size as for the feature vector calculation algorithm.

Points with the maximal (P_{max}) and minimal (P_{min}) value of mean or Gaussian curvature are found within the neighborhood. These points are used to create a triplet of vectors: $n, u = P_{max} - P, v = P_{min} - P$. The triplet can be used to calculate the signed volume $V_{s_{mean/Gauss}}$ of a parallelepiped, see Figure 5, as:

$$V_{s_{mean/Gauss}} = n \cdot (u \times v),$$

where the *mean* or *Gauss* index is used to distinguish the type of extrema used for calculation of u and v .

The sign of the volume is swapped for reflected parts, because the points P_{min} and P_{max} are reflected as

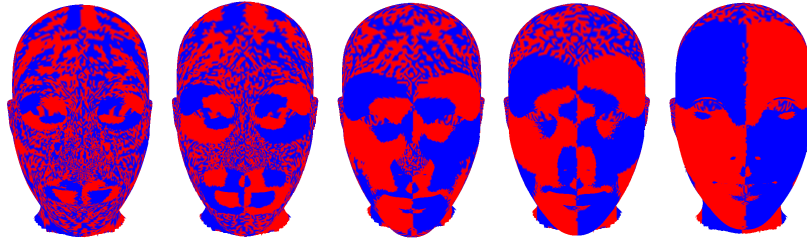


Figure 4: Comparison of neighborhoods for vector field flux. Blue color indicates negative flux, red is used for positive values. Neighborhood sizes are taken in percents of bounding box size. From left to right: 7%, 14%, 21%, 28% and 42%.

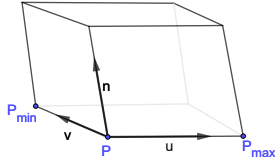


Figure 5: The triplet of vectors n , u and v and indicated signed volume of a parallelepiped.

well. However, due to the differences in the neighborhoods for left and right part, the positions of extrema are not guaranteed to be the same, which can lead to incorrect results. A possible solution is to divide the space into bins, eg. from the volumetric sphere centered around the point P . A simplified 2D scenario with only upper half of circle can be seen in Figure 6. Centroids of bins with the extremal averages of curvature are used to construct the vector triplet.

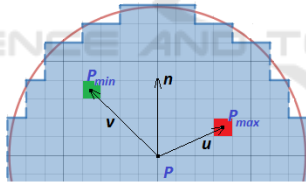


Figure 6: Bins around the center point P . Two bins with the extremal average curvatures are highlighted. Only upper, relevant half of circle is shown.

The curvature based solution for distinguishing left and right part behaves differently from the vector field based approach. The comparison of different neighborhood sizes can be seen in Figure 7. For sizes above 25%, the results are generally incorrect. This is caused by the large smooth areas with few details where small numerical error can change the vector triplet and results in incorrectly signed area.

3.3 Symmetry-aware Feature Vector

The signed representation of the neighborhood, as presented in subsections 3.1 and 3.2, is used to modify the feature vector. There are many ways how to modify the feature vector. We have tested several possibilities that either combine together the two represen-

tations (presented in subsections 3.1 and 3.2) or use them separately. Attaching the value to the end (or beginning) of the feature vector offered only a small amount of new information and did not improve the results. Therefore we have also considered multiplying the feature vector to include the sign together with the value. In some cases, further attaching other calculated value to the end of already multiplied feature vector further improved the results.

From all the tests, the ones that provide the best overall quality were selected. We compute the FPFH feature vector and use either F_s from the Vector Field, $V_{s_{mean}}$ from mean curvature or $V_{s_{Gauss}}$ from Gaussian curvature for modification. In the first step, we multiply FPFH by F_s and use one of the following modifications:

1. append F_s to the end
2. append $V_{s_{mean}}$ to the end
3. append F_s , $V_{s_{mean}}$ and $V_{s_{Gauss}}$ to the end
4. append $V_{s_{mean}}$ and $V_{s_{Gauss}}$ to the end

4 EXPERIMENTS AND RESULTS

We have used one of the current state-of-the-art methods, FGR (Zhou et al., 2016), as a baseline. This method uses FPFH feature vector to obtain the final transformation and in some cases, it leads to an incorrect alignment of two parts if they contain symmetric parts. For example, if we try to register two overlapping parts of the human head, the ears are detected in both parts with similar feature vectors, which affects the final transformation (see again Figure 1c).

4.1 Test Data

We need an automatic evaluation of registration quality. For this purpose, the correct registration has to be known. Therefore, instead of using scanned data, we have recreated partially overlapping parts from complete models. In our tests, We have used point clouds as well as their triangulations.

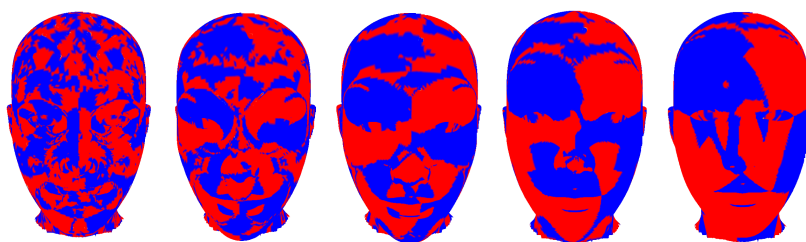


Figure 7: Comparison of neighborhoods for signed volume. Blue color indicates negative volume, red is used for positive values. Neighborhood sizes are taken in percents of bounding box size. From left to right: 7%, 14%, 21%, 28% and 42%.

To create overlapping parts from a complete model and simulate a scanning device, we use the following steps.

- The plane of symmetry is found.
- The plane is randomly rotated around the coordinate system axes in the interval $\langle -30^\circ, 30^\circ \rangle$. Larger rotation will cause too large overlaps which lead to easy registration.
- The plane is shifted in positive or negative direction of its normal vector. Shift distance depends on the model size and the size of the overlap we want to achieve.
- Vertices in one half-space of the plane are discarded

However, in this scenario, data can be matched 1:1 - e.g. there are points in both halves that can be exactly matched. To overcome this, we have added Gaussian noise to the data. In addition, for triangle meshes, Loop (Loop, 1987) subdivision scheme followed by a mesh simplification was used.

4.2 Comparison Metric

To compare the registration results, we have used a metric based on (Pottmann et al., 2006). From the two parts that are used for the registration, one (called model P) is at a fixed position and the other (called model Q) is transformed with a random translation and rotation. Inverse of this transformation will put the model to a position Q_1 in which it is correctly registered with model P .

We have obtained the registration matrix from the registration algorithm and transformed the model Q with this matrix which led to the position Q_2 . For a perfect registration, Q_1 and Q_2 are the same. To measure the deviation from a perfect registration, we compute distances between the corresponding vertices of Q_1 and Q_2 . The sum of distances is divided by the number of vertices and normalized by the data radius, making the value scale independent, although not necessarily in the $\langle 0, 1 \rangle$ interval.

Based on our observations, the resulting values can be interpreted as follows: Values under 0.1 can be considered a correct registration result. Values between 0.1 and 0.6 are registered very roughly, but the overall shape can be recognized. Values above 0.6 indicate incorrect registration and the result is on par with a random matrix.

4.3 Tests

The core of the tests is based on the FPFH descriptor. We have used several radii that are based on the average number of points that fall within. We have started with 10 points and ended with a neighborhood of the size 160 points, using a step of 10 points. From the number of points, we have calculated the average radius size of the geometry and this radius was used for FPFH. The radius was different for each tested model, depending on the model scale and sampling density.

In our experiments, we have used the same radius for both FPFH calculation and for the calculation of neighborhoods for the proposed methods. We have tested different sizes of neighborhoods as well. However, for smaller neighborhoods (< 10) the results were often similar to a flat surface. There were certain precision improvements with neighborhoods of larger size (> 160), but the computation times were longer. As a trade-off between quality and speed, we have selected using neighborhoods of the same size.

We have created an automated test scenario, where the input model is randomly divided into two overlapping parts (see subsection 4.1). For every split, we have computed metrics for every variation of the feature vector modification proposed in subsection 3.3. The basic solution taken from FGR was able to correctly register only about 40% of our input test cases, while the rest was registered incorrectly (with metric values being above 0.1).

We have conducted several thousand tests with different models of human heads and faces. For the tests, we have used a triangle mesh and a point cloud representation of the input model. The overall results were roughly the same for both approaches and correspond with averaged results. These overall averaged

Table 1: Comparison of successfully registered input cases based on different points count in the neighborhood.

Method	Size 10	Size 60	Size 150
-	41%	43%	34%
1	44%	42%	28%
2	48%	45%	33%
3	51%	50%	31%
4	55%	49%	36%

results are presented in Table 1. The method number in the first column of the table corresponds with the feature vector modification method number from subsection 3.3. The symbol “-” marks the original FGR method without any modification. The table shows the percentage of correct registrations for three different neighborhood sizes (10, 60 and 150). Note that the globally low success rate in general is caused by an automated data creation, which often leaves only a small overlap.

We have observed that with the increasing neighborhood size, the results were improving only to a certain threshold. The quality of the registration began to decrease for a neighborhood calculated from around 60 points, probably because the descriptor was constructed from a too large area. For a human head, it often means that a large part of the descriptor is based on smooth surfaces (cheeks, forehead or chin). In these cases, the basic FGR algorithm offers better results.

The visual comparison of results can be seen in Figure 8. The original data (Figure 8a) differs from the best registration result (Figure 8d) because of the data modification described in Subsection 4.1. The difference between Figure 8c and Figure 8d is mainly in the nose area. The two parts in Figure 8c are registered very roughly and there are many intersections of the two parts along their overlap. In Figure 8d the registration is correct with a smooth transition from one part to another. The missing parts are caused by the automated data creation.

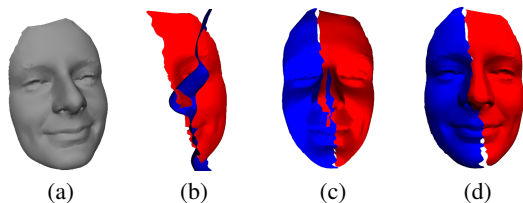


Figure 8: Visual comparison of results; a) Original data; b) FGR only, $error = 1.578$; c) The proposed registration, $error = 0.192$; d) The proposed registration, $error = 0.074$.

4.4 Limitations

The proposed algorithm has certain limitations. Some of them are globally related to the registration itself. If the overlap of two parts is too small, the resulting registration is often incorrect. The same goes for too much noise in the data.

The main problem of the proposed solution is selecting optimal feature vector modification. Depending on the data, one choice may be considerably better than others. This is currently solved manually, when the user has to check if the registration is correct. In future research, we would like to focus on this part and create an automated system that can distinguish incorrect registration automatically and eventually choose another feature vector. We have already experimented with solutions based on projections of geometry to 2D plane and comparison of projected depth values, but the results are currently not reliable.

Our current solution is only suitable for a limited set of data - scans of human heads. We have also tested general models with symmetries, however, the quality of registration was not globally improved with our algorithm.

5 CONCLUSIONS

An improvement of the registration for scanned data of human head was proposed. The solution can be implemented into existing registration algorithms as an extension of the currently existing feature vector. We have shown that augmenting a feature vector by our symmetry aware measures leads to a considerable improvement in registration success rate.

Currently, we do not have a single feature vector augmentation strategy that works best in all cases. If the best possible result is required, user interaction is necessary. The user must decide whether or not the registration is correct. This is far from ideal, although such solution is still faster than manually finding the transformation. Moreover, the decisions of correctness can be made by a layman, while a manual registration requires certain experience. In our future research, we would like to remove this limitation by using an automatic detection of registration correctness.

As a part of our future work, we would like to extend our proposed algorithm to general models. The current solution can be naturally applied to any models, but the improvement of registration unfortunately is not significant in the general case.

ACKNOWLEDGEMENT

This publication was supported by the project LO1506 of the Czech Ministry of Education, Youth and Sports under the program NPU I.

REFERENCES

- Bay, H., Ess, A., Tuytelaars, T., and Gool, L. V. (2008). Speeded-up robust features (surf). *Computer Vision and Image Understanding*, 110(3):346–359.
- Drost, B., Ulrich, M., Navab, N., and Ilic, S. (2010). Model globally, match locally: Efficient and robust 3d object recognition. In *2010 IEEE Computer Society Conference on Computer Vision and Pattern Recognition*, pages 998–1005.
- Elbaz, G., Avraham, T., and Fischer, A. (2017). 3d point cloud registration for localization using a deep neural network auto-encoder. In *2017 IEEE Conference on Computer Vision and Pattern Recognition (CVPR)*, pages 2472–2481.
- Foulds, H. and Drevin, G. R. (2011). Three-dimensional shape descriptors and matching procedures. In *WSCG '2011: The 19th International Conference in Central Europe on Computer Graphics, Visualization and Computer Vision, p. 1-8.*, pages 1–8.
- Gelfand, N., Mitra, N. J., Guibas, L. J., and Pottmann, H. (2005). Robust global registration. In *Proceedings of the Third Eurographics Symposium on Geometry Processing, SGP '05, Aire-la-Ville, Switzerland, Switzerland*. Eurographics Association.
- Guo, Y., Bennamoun, M., Soheli, F., Lu, M., Wan, J., and Kwok, N. M. (2016). A comprehensive performance evaluation of 3d local feature descriptors. *International Journal of Computer Vision*, 116(1):66–89.
- Holz, D., Ichim, A. E., Tombari, F., Rusu, R. B., and Behnke, S. (2015). Registration with the point cloud library: A modular framework for aligning in 3-d. *IEEE Robotics Automation Magazine*, 22(4):110–124.
- Jiaqi, Y., Zhiguo, C., and Qian, Z. (2016). A fast and robust local descriptor for 3d point cloud registration. *Information Sciences*, 346-347:163 – 179.
- Johnson, A. E. and Hebert, M. (1999). Using spin images for efficient object recognition in cluttered 3d scenes. *IEEE Transactions on Pattern Analysis and Machine Intelligence*, 21(5):433–449.
- Knopp, J., Prasad, M., Willems, G., Timofte, R., and Gool, L. V. (2010). Hough transform and 3d surf for robust three dimensional classification. In *Proceedings of the 11th European Conference on Computer Vision: Part VI, ECCV'10*, pages 589–602. Springer Berlin Heidelberg.
- Lin, B., Wang, F., Sun, Y., Qu, W., Chen, Z., and Zhang, S. (2017). Boundary points based scale invariant 3d point feature. *Journal of Visual Communication and Image Representation*, 48:136 – 148.
- Liu, H., Yan, J., and Zhang, D. (2006). A neural network strategy for 3d surface registration. In *Computational Science and Its Applications - ICCSA 2006*, pages 528–536. Springer Berlin Heidelberg.
- Loop, C. (1987). *Smooth Subdivision Surfaces Based on Triangles*. PhD thesis, Department of Mathematics, The University of Utah, Masters Thesis.
- Lowe, D. G. (2004). Distinctive image features from scale-invariant keypoints. *International Journal of Computer Vision*, 60(2):91–110.
- Maximo, A., Patro, R., Varshney, A., and Farias, R. (2011). A robust and rotationally invariant local surface descriptor with applications to non-local mesh processing. *Graphical Models*, 73(5):231 – 242.
- Pottmann, H., Huang, Q. X., Yang, Y. L., and Hu, S. M. (2006). Geometry and convergence analysis of algorithms for registration of 3d shapes. *International Journal of Computer Vision*, 67(3):277–296.
- Pottmann, H., Wallner, J., Yang, Y. L., Lai, Y., and Hu, S. M. (2007). Principal curvatures from the integral invariant viewpoint. *Computer Aided Geometric Design*, 24(8 - 9):428 – 442.
- Rusu, R. B., Blodow, N., and Beetz, M. (2009). Fast point feature histograms (fpfh) for 3d registration. In *Robotics and Automation, 2009. ICRA '09. IEEE International Conference on Robotics and Automation*, pages 3212–3217.
- Tombari, F., Salti, S., and Stefano, L. D. (2010). Unique signatures of histograms for local surface description. In *Proceedings of the 11th European Conference on Computer Vision Conference on Computer Vision: Part III, ECCV'10*, pages 356–369. Springer Berlin Heidelberg.
- Váša, L., Vaněček, P., Prantl, M., Skorkovská, V., Martínek, P., and Kolingerová, I. (2016). Mesh statistics for robust curvature estimation. *Computer Graphics Forum*, 35(5):271–280.
- Zhou, Q. Y., Park, J., and Koltun, V. (2016). Fast global registration. In *Computer Vision – ECCV 2016*, pages 766–782, Cham. Springer International Publishing.